Stress Distribution in a Packed Bed Above Raceway Cavities Formed by an Air Jet

The vertical stress profile in a packed bed above the cavities formed by an upward, high-velocity air jet is estimated from a force balance analysis and static pressure measurements. The objective is to understand and determine the forces responsible for maintaining the cavity roof. Such cavities, formed in an iron blast furnace, adjacent to the hot air blast emanating from the tuyere pipes, are called raceways. A net upward force provided by the gas pressure drag and the support from the bed walls holds the raceway roof in its position. Abrupt changes in the stress and the gas velocity are observed near the roof. The zero vertical stress is also found close above the roof but fluctuates vertically with the raceway size, which varies irreversibly following a cyclic change in the blast rate.

Vivek B. Apte
Terry F. Wall
John S. Truelove
Department of Chemical Engineering
University of Newcastle
Newcastle NSW 2308, Australia

Introduction

In the iron blast furnace, hot air with supplementary fuels is blown at a high velocity through a number of tuyere pipes located along the circumference of the lower part of the furnace. The blast momentum creates high voidage regions, called raceways, containing recirculating coke particles. A cold simulation of this phenomenon is illustrated in Figure 1, where a raceway is formed by blowing an air jet in a packed bed. In a blast furnace, gases (mainly CO and H_2) formed in the raceway region travel upward, reducing the iron oxide in the downcoming charge to metallic iron. The charge movement and the distribution of the reducing gases are substantially affected by the raceway geometry and therefore its relationship with the bed and the gas flow properties has been extensively studied (Apte, 1986; Apte et al., 1988; Burgess, 1985). For a prediction of the raceway geometry from first principles, information regarding the flow and stress condition around the raceway is necessary (Apte, 1986). The objective of this paper is to analyze the stresses responsible for maintaining the raceway roof in its position. A simplified model considered here, Figure 1, employs a vertical air jet to form a raceway. This enables a force balance along a known streamline coincident with the jet axis. The frictional properties of the packing materials required for the present calculations were measured by a standard method using a Jenike shear cell (Arnold et al., 1979). Due to the frictional support from the bed walls, increases in the packing height beyond a certain limit have little effect on the bed weight (Arnold et al., 1979), which in previous models (Szekely and Poveromo, 1975) has been assumed as an equivalent hydrostatic head.

The present simplified model has clarified our understanding of the forces balancing the raceway roof. The gas pressure drag and the support from the particle-wall friction are shown to hold the roof in equilibrium against the bed weight. The stress and the gas flow profiles change rapidly in the proximity of the roof. Beyond a few raceway diameters above the roof, the gas flow becomes uniform and the stress profile approaches that with no gas flow. The plane of zero vertical stress is located very close to the raceway roof, the location fluctuating vertically during the raceway hysteresis observed as flow is increased and then decreased. With increasing flow, the roof stress is upward; stress approaches zero with decreasing flow and finally becomes zero when the roof begins to collapse.

Derivation of Vertical Stress, σ_y, Equations

Consider a raceway formed by a vertical air jet issuing from a tuyere inserted centrally through the bottom face of a two-dimensional bed packed with granular solids, Figure 1. The

Correspondence concerning this paper should be addressed to T. F. Wall.
The present address of V. B. Apte is: Mechanical Engineering Department, University of Sydney, Sydney NSW 2006, Australia.

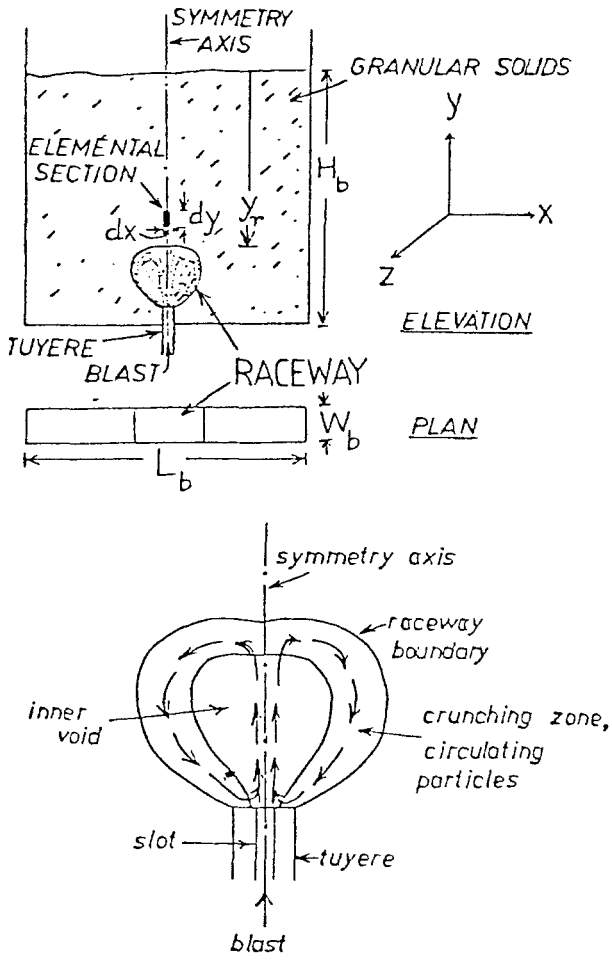

Figure 1. Two-dimensional raceway model for balancing vertical forces in packed bed.

raceway boundary is defined as the stationary bed/moving particle interface. Inside this boundary, particles circulate in a crunching zone that surrounds the central region of higher voidage. This arrangement simplifies balancing of vertical forces in the bed along the streamline coincident with the tuyere axis. On this y axis, an elemental section with a height dy, length dx, and width W_b is subjected to downward and upward forces balanced as follows (terms are defined in the notation):

$$\sigma_y(dxW_b) + \rho_b g(dxW_b dy) = (\sigma_y + d\sigma_y)(dxW_b) + dP(dxW_b) + S \quad (1)$$

The terms on the lefthand side of this equation, in order, are the resultant force and the elemental weight. The terms on the righthand side are the reaction to the resultant force, the upward gas pressure drag, and the particle-wall frictional support. This support is calculated from the upward shear forces acting on the vertical faces of an element with the same cross-sectional area as the bed (L_bW_b), and a height dy as follows:

$$S = \frac{(2\tau_w W_b dy + 2\tau_w L_b dy)}{L_b W_b} dxW_b \quad (2)$$

Simplification of Eq. 2 and its substitution in Eq. 1 yields

$$d\sigma_y = \rho_b g dy - dP - 2\tau_w\left(\frac{1}{L_b} + \frac{1}{W_b}\right)dy \quad (3)$$

The coefficient of friction between the bed walls and the solids has been defined as (Arnold et al., 1979)

$$\mu_w = \frac{\tau_w}{\sigma_z} = \frac{\tau_w}{\sigma_x} = \tan\phi_w \quad (4)$$

assuming equal horizontal stresses σ_x and σ_z. A lateral pressure coefficient K_j is defined below and can also be expressed as a function of the angle of internal friction (Arnold et al., 1979), δ.

$$K_j = \frac{\sigma_x}{\sigma_y} = \frac{\sigma_z}{\sigma_y} = \frac{(1 - \sin\delta)}{1 + \sin\delta)} \quad (5)$$

Using Eqs. 4 and 5, Eq. 3 can be rearranged to give a first-order, linear differential equation for σ_y above the raceway roof

$$\frac{d\sigma_y}{dy} = \rho_b g - \frac{dP}{dy} - C\sigma_y \quad (6)$$

This is the momentum equation for the gas-solid mixture with the dyamic terms neglected. The constant C in Eq. 6, called a *bed support factor*, is defined as

$$C = 2\mu_w K_j\left(\frac{1}{L_b} + \frac{1}{W_b}\right) \quad (7)$$

For a uniform C in the bed and $dP/dy = fn\,(y)$, Eq. 6 is solved with the boundary condition $\sigma_y = 0$ at $y = 0$, the bed surface, to obtain

$$\sigma_y = \frac{\rho_b g}{C}(1 - e^{-Cy}) - e^{-Cy}\int_0^y e^{Cy}\frac{dP}{dy}dy \quad (8)$$

The first term on the righthand side of Eq. 8 is the effective bed weight, while the second term represents the upward gas pressure drag. The bulk properties ρ_b, ϵ_b, μ_w, δ, K_j, and C appearing in this treatment are assumed uniform in the bed

For a uniform gas flow, that is, a constant dP/dy in the bed, Eq. 8 reduces to

$$\sigma_y = \frac{1}{C}\left(\rho_b g - \frac{dP}{dy}\right)(1 - e^{-Cy}) \quad (9)$$

The stress σ_y is zero when the pressure drop equals the weight of the bed, corresponding to the minimum fluidization condition. For a no gas flow situation, that is, a static bed without a raceway, Eq. 8 takes the form

$$\sigma_y = \frac{\rho_b g}{C}(1 - e^{-Cy}) \quad (10)$$

This is the classical Janseen's equation (Janseen, 1895), assuming a constant σ_y over any horizontal cross section. For deep

beds, as $y \to \infty$, Eq. 10 becomes

$$\sigma_y = \frac{\rho_b g}{C} \tag{11}$$

This limiting σ_y value is reached at a bed depth of approximately five times the container diameter (Arnold et al., 1979).

Significance of C

The *bed support factor, C*, defined in Eq. 7 would be larger for materials with a higher coefficient of wall friction and smaller for wider beds with less wall effect. Thus, C may be considered a measure of the wall support given to the bed weight; a larger C would imply more wall support and a smaller effective bed weight.

From Eq. 10, $\lim_{C \to 0} \sigma_y = \rho_b g y$, indicating that for $C = 0$, the bed weight would be transmitted as an equivalent hydrostatic head and the bed stresses would be isotopic.

As an alternate physical interpretation of C using Eq. 11, the reciprocal of C may be said to represent the characteristic, limiting packed bed depth (Arnold et al., 1979) $\simeq 5\ W_b$.

The factor C is thus determined by the materials used for the bed and the containing walls. The present experiments used monosize plastic and glass beads in two-dimensional enclosures as described in the next section. A practical system (e.g., a blast furnace) has coke of varying sizes with walls far enough removed from the raceway that the wall support can be neglected.

Uncertainties in estimating C

The calculation of C from Eq. 7 involves estimating an appropriate value of K_j, over which there is a considerable conjecture in the literature (Apte, 1986) due to an insufficient understanding of the properties of granular materials. A number of expressions have been proposed for K_j, including a prescribed value of 0.4 for most materials (Arnold et al., 1979). K_j has been reported to be an anisotropic property (Delaplaine, 1956; Glastonbury and Bratel, 1966), also affected by the conditions under which the packing is done, ρ_b, ϵ_b, and the impact loads and vibrations (Babarykin, 1962).

Static Pressure Measurement

Estimation of σ_y from Eq. 8 requires measurement of the static pressure profile in the bed. Rectangular enclosures, Figure 1, 570 mm wide × 920 mm high with inside widths of 14, 20, and 30 mm, made of 6 mm thick transparent plastic sheets were used for the two-dimensional experiments. A central air entry (tuyere) protruded 40 mm into the enclosure through its bottom face. The tuyeres, designed to fit into the 14, 20, and 30 mm wide enclosures had 1.05, 1.4, and 0.95 mm slotted openings, respectively, running across the bed width. Circular tuyeres with 6 and 7.8 mm ID were also used to see the effect of tuyere geometry. On the face of the enclosure, 1.65 mm dia. holes were drilled for static pressure measurement. The enclosure was filled to a depth of approximately 500 mm with granular plastic or glass material; Table 1 lists the properties. At a number of increasing blast flow rates, measurements were taken of the raceway size (which grows with the flow), and of the static pressure profile in the raceway and the bed at a 5 mm spacing along the tuyere axis. For fluctuating pressure readings near the raceway boundary, an average value over a period of 60 s was taken. Measurements were also taken for a raceway formed after a further increase in the blast rate followed by a decrease to the same flow rate; the raceway now formed was bigger than the one at the same blast rate when the flow was increasing. The hysteresis in the raceway phenomenon has reported previously (Apte et al., 1988). It will be shown that for such raceways formed at the same flows but during the increasing and decreasing paths of a flow cycle, the stress at the raceway roof differs, as do the size and the flow distribution through the boundary (Apte et al, 1988). The gas velocities were sufficiently low that the bed above the raceway did not fluidize.

Measurements on three-dimensional raceways were made in a 0.15 m wide × 0.15 m long × 0.25 m tall plastic enclosure, filled to a depth of 0.2 m with granular material. A circular tuyere was inserted 20 mm vertically through the bottom face of the box, adjacent to one of the walls to obtain raceway visibility.

Bulk Solids Properties Measurement

Table 1 gives the measured values of the physical properties of the solids required for the present analysis. The particle density ρ_p was calculated by measuring the volume of a lighter liquid displaced by a known mass of the solids. The bulk density ρ_b of

Table 1. Bulk Solids Properties

Material Code	Particle Shape, Dimensions mm	D_p mm	ρ_p kg/m^3	ϕ_w deg	μ_w	δ deg	K_j Eq. 5	W_b mm	ρ_b kg/m^3	ϵ_b Eq. 12	C Eq. 7 m^{-1}
PL1, plastic	Cyl.							14	467.0	0.496	9.86
	dia. = 4	3.0	926	16.2	0.29	38.0	0.238	20	479.0	0.479	7.04
	ht. = 2							30	487.0	0.475	4.6
								150	487.0	0.475	1.84
PL2, plastic	Cubical							14	755.2	0.4504	10.98
	3 × 3 × 5	3.46	1,374	21.3	0.39	42.1	0.197	20	766.7	0.4421	7.84
								30	773.9	0.4368	5.12
								150	773.9	0.4368	2.05
GL3, glass	Spherical							14	1,560.0	0.388	9.99
	3.0	3.0	2,550	12.4	0.22	31.2	0.318	20	1,562.0	0.387	7.14
								30	1,578.0	0.381	4.66
								150	1,578.0	0.381	1.87

the freely packed materials was measured in the 14, 20, 30, and 150 mm wide enclosures. Voidage is then calculated from

$$\epsilon b = 1 - \rho b \rho p \quad (12)$$

The frictional properties δ and ϕ_w were measured by the standard Jenike shear cell method (Arnold et al., 1979); μ_w, K_j, and the bed support factor C are then calculated from Eqs. 4, 5, and 7, respectively. A 33% error band on these C values is estimated due to the uncertainties in K_j discussed earlier.

σ_y Computation—A Case Study

Table 2 presents a summary of all the experiments, including the material used, the enclosure and tuyere geometries, the flow condition, the raceway size, and the calculated σ_y profile. Let us consider run 6 in Table 2 to demonstrate computation of σ_y using Eq. 8 and the static pressure measurements.

Profiles of static pressure and its gradient

Figure 2 shows the measured static pressue profile along the tuyere axis in the flow direction. The pressure increases inside the raceway, reaching a maximum value of 1,650 Pa gauge at the impaction point of the jet on the packed bed (i.e., the inner boundary of the crunching zone), due to the conservation of kinetic energy into pressure energy, as at a stagnation point. Outside the raceway, within a distance of 0.025 m from this point, the pressure drops sharply to about 650 Pa. Beyond ~0.18 m from the tuyere exit, the pressure decreases linearly, indicating a uniform flow.

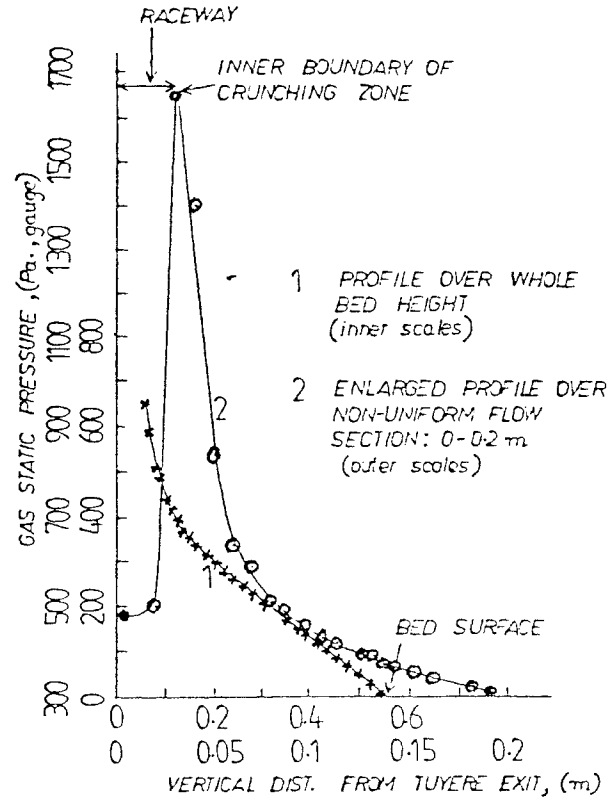

Figure 2. Measured static pressue along tuyere axis.

Table 2. Data for Points 1 to 21, Figure 6

Point No.	Material, Table 1	ρ_b kg/m³	Bed W_b m	Bed L_b m	Bed y_r m	Tuyere D_t mm	Raceway D_r m	Stresses σ_r Pa	Stresses Dist. of $\sigma_y = 0$ from Raceway Roof mm	Stresses Dist. of $\sigma_{y,max}$ from Raceway Roof mm	Flow Condition M g/s
1	PL1	467	0.014	0.573	0.483	14 × 1.05 slot	0.04	−217	3.9	133	3.64
2	PL1	467	0.014	0.573	0.465	14 × 1.05 slot	0.06	−151	4.9	125	4.28
3	PL1	479	0.0196	0.573	0.505	19.6 × 1.4 slot	0.021	−237	4.6	99	3.43
4	PL1	479	0.0196	0.573	0.495	19.6 × 1.4 slot	0.028	−72	1.5	95	4.01
5	PL1	479	0.0196	0.573	0.485	19.6 × 1.4 slot	0.037	−165	3.9	100	4.67
6	PL1	479	0.0196	0.573	0.485	19.6 × 1.4 slot	0.041	−178	5.3	120	5.32
7	PL1	479	0.0196	0.573	0.465	19.6 × 1.4 slot	0.058	−12	0.5	115	6.04
8	PL1	479	0.0196	0.573	0.455	19.6 × 1.4 slot	0.065	−45	2.2	107	6.77
9	PL1	479	0.0196	0.573	0.474	6 ID	0.051	−50	2.6	94	4.78
10	PL1	479	0.0196	0.573	0.45	6 ID	0.075	−5	0.5	92	6.04
11	PL1	487	0.03	0.573	0.495	30 × 0.95 slot	0.032	−493	5.7	100	8.25
12	PL1	487	0.03	0.573	0.485	30 × 0.95 slot	0.04	−281	4.7	110	9.31
13	PL1	487	0.03	0.573	0.48	30 × 0.95 slot	0.045	−166	3.9	105	$M\uparrow$ 10.2, then $\downarrow$ to 9.31
14	PL1	487	0.03	0.573	0.483	6 ID	0.045	−217	4.3	70	6.65
15	PL1	487	0.15	0.15	0.195	6 ID	0.048	−89	1.5	30	6.04
16	PL1	487	0.15	0.15	0.19	6 ID	0.05	−193	3.8	30	6.04
17	PL1	487	0.15	0.15	0.205	7.85 ID	0.035	−357	3.4	30	6.05
18	PL1	487	0.15	0.15	0.195	7.85 ID	0.043	+84	—	19	$M\uparrow$ 8.3, then $\downarrow$ to 4.75
19	GL3	1560	0.014	0.573	0.48	14 × 1.05 slot	0.035	+319	—	100	3.64
20	GL3	1560	0.15	0.15	0.215	6 ID	0.035	+247	—	30	6.04
21	PL2	766.7	0.0196	0.573	0.469	6 ID	0.058	−460	8.0	99	6.65

Slopes of the pressure profile are calculated to obtain the pressure gradient profile above the raceway roof, Figure 3. The dP/dy decreases by nearly a factor of 50 from its maximum value at the raceway roof (≃40,000 Pa/m) to ≃800 Pa/m at a distance of 0.15 m, beyond which the gradient becomes constant. The U_y velocity profile is then calculated from the well-accepted, semiempirical Ergun equation (Ergun, 1952), which expresses the pressure drop in a packed bed as a sum of the viscous and inertial loss terms as follows:

$$\frac{dP}{dy} = \frac{150(1-\epsilon_b)^2\mu U_y}{\epsilon_b^3 D_p^2} + \frac{1.75(1-\epsilon_b)\rho_b U_y^2}{\epsilon_b^3 D_p} \qquad (13)$$

The values of ϵ_b and D_p, assumed uniform in the bed, are taken from Table 1. It is clearly seen from Figure 3 that the velocity near the raceway roof is much higher than the measured minimum fluidization velocity of 0.76 m/s. This is certainly so for the roof to be supported by the upward gas flow. Up to ~0.15 m from the roof, the inertial U_y^2 term in Eq. 13 is dominant.

The σ_y profile

Substituting the computed pressure gradient profile in Eq. 8, the σ_y profile along the bed depth is estimated as shown by curve 1 in Figure 4. A value of C equal to 7.04 m^{-1} was taken from Table 1. The σ_y increases at a decaying rate from 0 Pa at the bed surface to a maximum of ~502 Pa at a depth of 0.365 m. Beyond this point, within a distance of 0.12 m, σ_y rapidly decreases, attaining a negative value (i.e., upward direction) at the raceway roof ($\sigma_y = -178$ Pa). The zero stress is situated 5 mm above the roof. As the raceway roof is held in equilibrium due to the opposing forces—that is, the effective bed weight and the upward drag due to the gas flow—one would expect σ_y to be either zero or negative. The rapid decrease in σ_y and the reversal of its direction near the roof are due to the high pressure gradients in this region, Figure 3. The σ_y distribution without gas flow calculated from Eq. 10 is represented in Figure 4 by curve 2; when compared with curve 1, it is seen that the stresses in the upper part of the bed are relatively unaffected by the flow. It is only in a small region near the raceway roof that rapid changes in the gas flow and the bed stresses occur.

Sensitivity of σ_r to C and dP/dy

The ultimate aim is to compute σ_r from Eq. 8. This requires a value of C, which is subject to uncertainties in estimating K_j. To

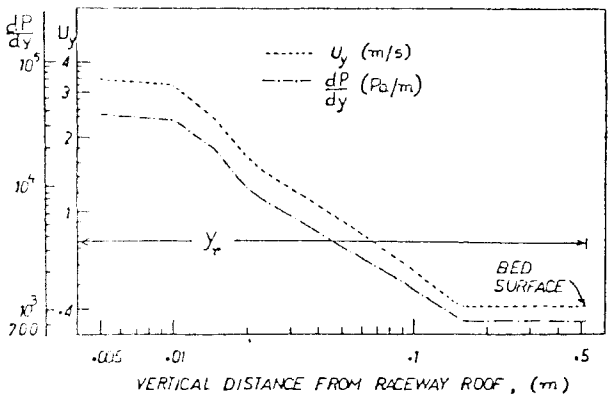

Figure 3. Pressure gradient and velocity profiles.

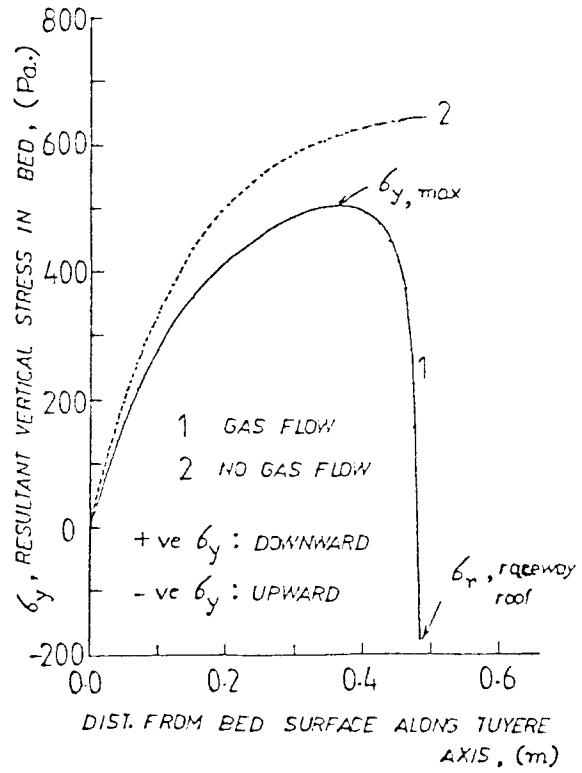

Figure 4. Vertical stress, σ_y, profile along tuyere axis.

clarify the effect of C on σ_r, Eq. 8 is solved for C, assuming σ_r equal to zero. *Let us denote this C as C_m.* For the present case, C_m is calculated to be 4.72 m^{-1}, whereas using the measured C of 7.04 m^{-1} (Table 1), σ_r is equal to −178 Pa (Figure 4). Thus, a comparison between the C_m (calculated) and C (measured) values summarized below can serve as an index of the stress condition at the raceway roof:

$C_m = C \quad \sigma_r = 0$

$C_m < C \quad \sigma_r < 0$, i.e., upward

$C_m > C \quad \sigma_r > 0$, i.e., downward

The last is physically not possible as the raceway would collapse.

The σ_y calculation, Eq. 8, also requires a measured dP/dy profile. The pressure profile, Figure 2, shows that 70% of the total pressure drop occurs only within 10% of the bed height from the raceway roof. Therefore the dP/dy values in this region will dominate the integral pressure drag term in Eq. 8. These pressure gradients may be subject to errors due to their calculation from the time-averaged measurements of the fluctuating pressures at and near the raceway roof. The fluctuations are severe for raceways formed in packings of heavier glass particles. The assumption of a uniform velocity between consecutive pressure tappings as well as across the tappings would introduce a further error in the dP/dy estimation.

For the present example, the sensitivity of σ_r to the pressure gradients within 20 mm from the raceway roof is shown in Figure 5. With a 33% error band on dP/dy (equivalent to a total

100% variation) the following changes are observed:

- σ_r computed using $C = 7.04\ m^{-1}$ varies from 0 to -450 Pa
- the location of $\sigma_y = 0$ shifts upward by 8.35 mm from the raceway roof
- C_m decreases from 7.04 to 2.7 m^{-1}

The error in the calculation of C_m due to measurement of dP/dy is estimated to be 33%.

σ_y Profile for Various Raceways

σ_r and $\sigma_{y,max}$

Figure 6 depicts σ_r for various raceways in terms of a comparison between C and C_m. Details regarding points 1 to 21 in this figure are given in Table 2. The error band on C_m is not shown to maintain clarity. It is seen from Table 2 that for raceways formed with a continuously increasing flow, σ_r is upward (i.e., $C_m < C$) irrespective of the bed and tuyere geometries. The unrealistic downward σ_r for cases 19 and 20 ($C_m > C$) may be explained from the error in estimating dP/dy near the roof. For all cases, the location of zero σ_y is close to the roof (a maximum of 8 mm above the roof for point 21). The negative C_m values, points 16 and 17, indicate that the assumption of a zero σ_r is not true in these cases.

In the σ_y profile of Figure 4, the maximum downward value is located 120 mm above the raceway roof. An examination of Table 2 reveals that for a particular bed and packing, this distance remains more or less unchanged for raceways formed with increasing flows.

Effect of tuyere and bed geometry

Points 7 and 10 in Figure 6 correspond to the raceways formed with a slotted and a circular tuyere, respectively, all other conditions remaining the same. Considering the error analysis discussed earlier, σ_r may be said to be independent of the tuyere used. This can also be said for points 16 and 17. Since

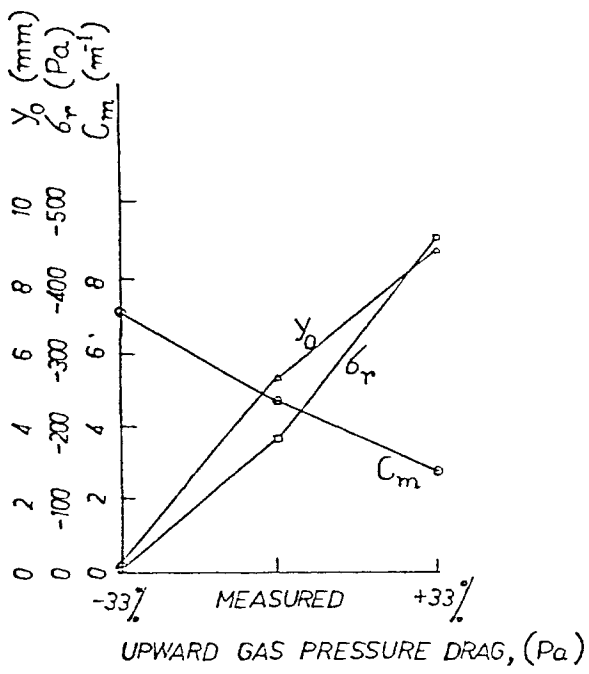

Figure 5. Sensitivity of estimated stresses near raceway roof to dP/dy in that region.

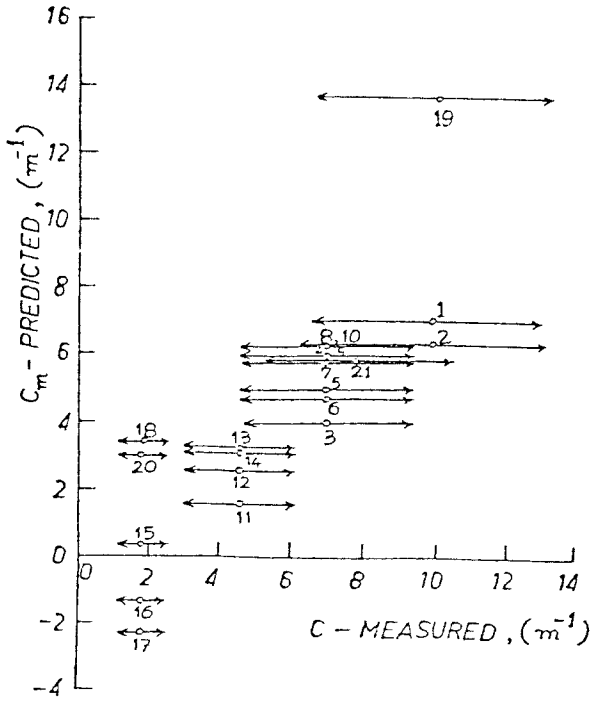

Figure 6. Measured, C, and predicted, C_m, bed support factor, indicating stress condition at raceway roof.

See Table 2 for details on points 1 to 21
Arrows show error on band C

the present analysis only applies above the roof and assumes no variation in z direction, the tuyere geometry would not be expected to enter the stress computations, as supported by the above observations.

Examining Figure 6, C_m is seen to decrease with an increasing bed width when the following groups of points are compared: 1 and 2, 3 to 10, 11 to 14, and 15 to 17—which correspond to 14, 20, 30, and 150 mm wide beds, respectively (Table 2). A similar trend is observed between points 19 and 20. This variation of C_m with bed width agrees with the definition of C.

The C_m values in Figure 6 for identical bed geometries are averaged and compared to C in Figure 7 for various materials. The agreement between C and C_m is reasonable considering their overlapping error bands. Also, the previously discussed trends of decreasing C and C_m values with increasing bed width are obvious here.

For a three-dimensional raceway, following the approach used in the section on derivation of the stress equations, an expression identical to Eq. 8 can be derived for σ_y. The definition of C would remain the same as in Eq. 7. The C here would be much smaller than that for a two-dimensional case due to a decreased wall effect; see Table 1, last column: C corresponding to the 150 mm wide bed.

Effect of raceway hysteresis

Raceways are found to increase in size with the blast at a greater rate than they subsequently decrease as the blast is reduced (Apte, 1986). This irreversible behavior following a cyclic change in the blast is called hysteresis; it is caused by the interlocking between the individual particles, which restricts

their freedom of movement (Apte, 1986). Points 12 and 13 in Figure 6 correspond to the raceways formed at the same blast rate but in the increasing and decreasing flow sections of a hysteresis cycle, respectively, Table 2. The upward σ_r here decreases from −281 to −166 Pa.

The raceways of points 17 and 18 are formed similarly following an increasing and a decreasing flow, respectively, but at different blast rates. Here, an inversion of σ_r (−357 to + 84 Pa) is seen.

Based on these and previous observations in this work, a hypothesis is now proposed for the variation of σ_r with flow, during a raceway hysteresis.

Figure 8a qualitatively shows the change in the raceway size with a cyclic variation of the blast rate (Apte, 1986). The dots above raceways 1–5, Figure 8b, indicate the shifting location of the zero σ_y.

For tall beds, Eq. 11, the effective bed weight on the raceway roof will have a limiting value of $\rho_b g/C$ for all cases, 1 to 5. In the increasing flow section, 1–2, Figure 8a, σ_r is negative, that is, upward, and so the zero σ_y is located above the roof.

In line 2–4 of Figure 8a, as the raceway size remains unchanged despite a decreasing blast flow, the gas velocity at the raceway roof (or the gas pressure drag supporting the roof) decreases. This decreasing drag, balanced against a constant bed weight, will result in a σ_r (upward) decreasing for the successive raceways 2–4. Accordingly, the $\sigma_y = 0$ location for these raceways will descend closer to the roof, Figure 8b.

In line 4–5 of Figure 8a, as the raceway collapses with a decreasing blast rate, the zero σ_y is situated at the roof, Figure 8b, raceway 5. Estimation of σ_y values near the roof is not possible in this case due to the highly fluctuating pressures near the raceway boundary, which itself is quite unstable and ill-defined. This observation would further support the existence of a zero roof stress during section 4–5 of Figure 8a.

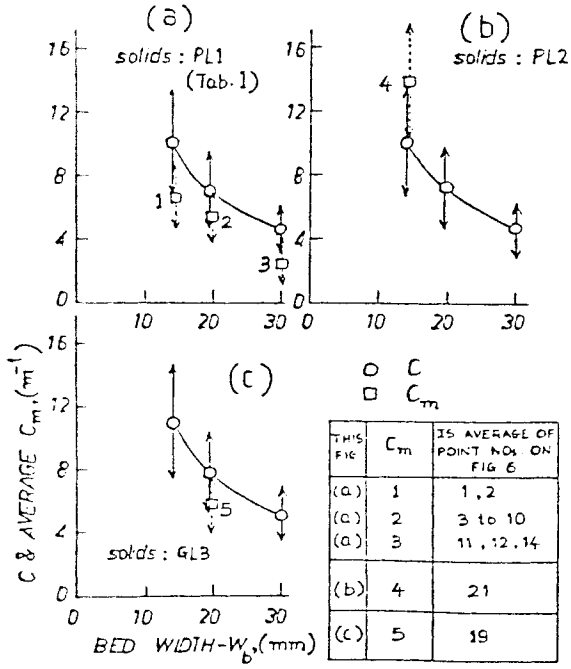

Figure 7. Variation of C and C_m with bed width.
Arrows show error bands

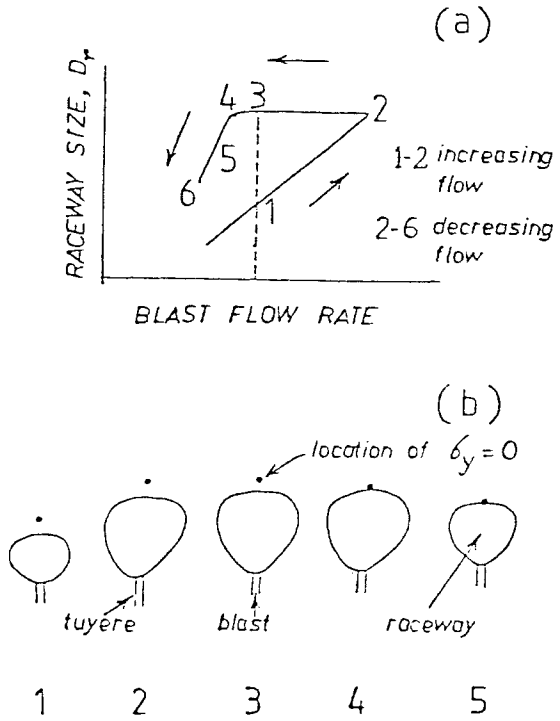

Figure 8. Transient behavior of σ_y during a hysteresis cycle.
(a) Raceway hysteresis (b) Shifting location of $\sigma_r = 0$ during hysteresis; raceways 1–5 correspond to points 1–5 in (a)

Notation

C = bed support factor calculated from geometry and material properties, Eq. 7, m^{-1}
C_m = bed support factor estimated from force balance model, assuming $\sigma_r = 0$, m^{-1}
D_p = diameter of sphere having same surface area as that of particle, m
D_r = raceway depth along blast direction, m
D_t = tuyere inside diameter, m
g = gravitational acceleration, m · s^{-2}
H_b = total bed depth, m
H_r = raceway dimension perpendicular to D_r, m
K_j = lateral pressure coefficient = $\sigma_x/\sigma_y\,\sigma_z/\sigma_y$
L_b = bed length along x axis, m
M = blast mass flow rate, kg · s^{-1}
P = gas static pressure, Pa, gauge
S = support due to particle-wall friction, N
U_r = U_y at raceway roof, m · s^{-1}
U_t = mean velocity at tuyere exit, m · s^{-1}
U_y = superficial vertical gas velocity in bed, m · s^{-1}
W_b = inside bed width along z axis, m
W_s = width of tuyere slot opening, m
x, y, z = distance along horizontal, vertical, and perpendicur (to plane of paper) axis, m
y_o = distance between raceway roof and zero vertical stress, m
y_r = bed depth up to raceway roof, m

Greek letters

δ = effective angle of internal friction for solids, deg
ϵ_b = packed bed voidage
ϕ_w = kinematic angle of friction between bulk solids and bed wall, deg
μ = kinematic viscosity of air, Pa · s
μ_s = coefficient of internal friction of solids = tan (δ)
μ_w = coefficient of friction between bulk solids and bed wall = tan (ϕ_w)

ρ_a = density of air, kg · m^{-3}
ρ_b = bulk density of packing in bed, kg · m^{-3}
ρ_p = particle density, kg · m^{-3}
$\sigma_r = \sigma_y$ at raceway roof, Pa
$\sigma_x, \sigma_y, \sigma_z$ = stresses in bed along x, y, and z directions, Pa
τ = shear stress between bulk solids and bed wall, Pa
$\sigma_{y,max}$ = maximum σ_y, Pa

Literature Cited

Apte, V. B., "Geometrical and Aerodynamic Characteristics of Cavities formed by Jets in Packed Beds," Ph.D. thesis, Chem. and Materials Eng. Dept., Univ. Newcastle, Australia (July, 1986).

Apte, V. B., T. F. Wall and J. S. Truelove, "Gas Flows in Raceways Formed by High-Velocity Jets in a Two-Dimensional Packed Bed," *Chem. Eng. Res. Des.*, **66,** 357 (1988).

Arnold, P. C., A. G. Mclean, and A. W. Roberts, "Bulk Solids—Storage, Flow, and Handling," TUNRA Limited, Univ. Newcastle, Australia (1979).

Babarykin, N. N., "Pressure of Charge and Gas in the Blast Furnace," *Steel in the USSR* (Eng. trans. of *Stal*), 667, (Sept. 1962).

Burgess, J. M., "Fuel Combustion in the Blast Furnace Raceway Zone," *Prog. Energy Comb. Sci.*, **11,** 61, (1985).

Delaplaine, J., "Forces Acting in Flowing Beds of Solids," *AIChE. J. 2* (1), 127 (March, 1956).

Ergun, S., "Fluid Flow Through Packed Columns," *Chem. Eng. Prog.*, **48,** 89 (1952).

Glastonbury, J., and P. Bratel, "Pressures in Contained Particle Beds from a Two-Dimensional Model," *Trans. Inst. Chem. Engrs.*, **44,** T128 (1966).

Janseen, H., "Tests on Grain Pressures in Silos," *Zeitschrift des Vereines deutscher Ingenieure, 39* (35), 1045 (1895).

Szekely, J., and J. Poveromo, "A Mathematical and Physical Representation of the Raceway Region in the Iron Blast Furnace," *Met. Trans B, 6B,* 119 (March, 1975).

Manuscript received July 12, 1989, and revision received Jan. 2, 1990.

Errata

In the paper titled "A Unified Approach for Moments in Chromatography" by W.-C. Lee, S.H. Huang, and G.T. Tsao (**34,** December 1988, p. 2083), the following corrections are made in Table 1:

In Model II, k in f_2 and f_3 expressions should read K.

In Model IV, the leading term for f_3 should read 2/315 instead of 1/315. In the same model, the definition of fluid film mass transfer coefficient k_f in the boundary condition is adopted from Ruthven (1984, p. 238), and is not consistent with those in other models. k_f should be replaced by $(d_p k_f)/(6 \rho_p)$ in the boundary condition and in all the derived expressions.

The errors were kindly pointed out by Rhonda M. Brand and Rane L. Curl.